From gaseous HCN to nucleobases at the cosmic silicate dust surface: an experimental insight into the onset of prebiotic chemistry in space

PCCP
Physical Chemistry Chemical Physics

Accepted Manuscript

This article can be cited before page numbers have been issued, to do this please use: R. Santalucia, M. Pazzi, F. Bonino, M. Signorile, D. Scarano, P. Ugliengo, G. Spoto and L. Mino, *Phys. Chem. Chem. Phys.*, 2022, DOI: 10.1039/D1CP05407D.

View Article Online
DOI: 10.1039/D1CP05407D

ARTICLE

From gaseous HCN to nucleobases at cosmic silicate dust surface: an experimental insight into the onset of prebiotic chemistry in space

Received 00th January 20xx,
Accepted 00th January 20xx

DOI: 10.1039/x0xx00000x

Rosangela Santalucia,[ab] Marco Pazzi,[a] Francesca Bonino,[ab] Matteo Signorile,[ab] Domenica Scarano,[ab] Piero Ugliengo,* [ab] Giuseppe Spoto,* [ab] and Lorenzo Mino [ab]

In memory of Professor Gianmario Martra

HCN in gas form is considered as a primary nitrogen source for the synthesis of prebiotic molecules in extraterrestrial environments. Nevertheless the research mainly focused on the reactivity of HCN and its derivatives in aqueous systems, often using external high-energy supply in form of cosmic rays or high energy photons. Very few studies were devoted to the chemistry of HCN in gas phase or at gas/solid interphase, although they represent the more common scenarios in the outer space. In this paper we report about the reactivity of high purity HCN in the 150-300 K range at the surface of amorphous and crystalline Mg_2SiO_4 (forsterite olivine), i.e. of solids among the constituents of the core of cosmic dust particles, comets, and meteorites. Amorphous silica and MgO were also studied as models representative of the Mg_2SiO_4 structural building blocks. IR spectroscopic results and the HR-MS analysis of the reaction products revealed the $Mg^{2+}O^{2-}$ acid/base pairs at the surface of Mg_2SiO_4 and MgO to be key in promoting the formation of HCN oligomers along with imidazole and purine compounds, already in very mild temperature and HCN pressure conditions, i.e. in absence of external energetic triggers. Products include the adenine nucleobase, a result which supports the hypothesis that prebiotic molecular building blocks can be easily formed through surface catalytic processes in absence of high-energy supply.

Introduction

Hydrogen cyanide is nowadays considered as a key ingredient for the synthesis of organic molecules relevant to the origin of life. After the early evidence given in 1961 by Oró *et al*. of the spontaneous synthesis of adenine from its solutions in ammonia,[1] attention was focused on the possible role of HCN in the formation of nucleobases and other biomolecules under conditions simulating the primordial terrestrial environment.[2] The detection of purine and pyrimidine compounds in carbonaceous chondrites (i.e., in primitive meteorites) then prompted the hypothesis that canonical nucleobases may also have formed in an extraterrestrial environment during the early stages of our solar system.[3, 4] Since HCN is a ubiquitous molecule in the universe,[5-12] it is believed that it could represent the major nitrogen source for the synthesis of chemical species of prebiotic concern. Complex molecules in space can be formed directly in gas-phase or at solid surfaces. Amorphous and crystalline silicates, comprising olivines $(Mg,Fe)_2SiO_4$ and pyroxenes $(Mg, Fe)_2Si_2O_6$, are the major constituents of planets, satellites, comets, meteorites, and asteroids, as well of the core of the dust grains present in the interstellar medium.[13-15]

Such minerals could hence have played a crucial role in the development of molecular complexity acting as heterogeneous catalysts.[16, 17] On this basis, many studies have been devoted to the investigation of the reactivity of liquid formamide in presence of different minerals,[18] as formamide (an HCN hydrated form) is also considered a potential precursor of primordial nucleobases and it is much easier to produce and handle than HCN in standard laboratory conditions. It is finally noticeable that most of the experiments in this field are performed by using thermal processing (T >> 300 K) or UV/protons irradiation as energetic input in order to simulate the harsh astrophysical context.[19-23] On the contrary, studies focused on the role played by mineral surfaces in adsorbing and concentrating gas phase HCN and in catalysing its transformation into products of prebiotic relevance without external energy inputs are lacking. Aiming to contribute to fill this gap, we have studied the interaction of pure HCN with the surface of a synthetic Mg-silicate with end-member stoichiometry (Mg_2SiO_4) in amorphous (AMS) and crystalline (CMS or forsterite) forms, assumed as laboratory models of cosmic silicate core dust particles.[24] To attain a better knowledge of the HCN/Mg_2SiO_4 chemistry, we also studied the interaction of HCN with amorphous SiO_2 and MgO, two reference solids whose surface properties have been extensively investigated in the past and whose structures contain the same structural building blocks of AMS and CMS (SiO_4 tetrahedra, and Mg^{2+} and/or $(Mg^{2+}O^{2-})_x$ species).[25-28] A key point of this investigation was the production of pure HCN and its dosage on the solid samples in safe and fully controlled

[a] Department of Chemistry, University of Turin, 10125, Turin, Italy.
[b] Nanostructured Interfaces and Surfaces (NIS) Interdepartmental Centre, 10125, Turin, Italy.

† Electronic Supplementary Information (ESI) available: materials and methods, HR-MS spectra of amorphous and crystalline Mg_2SiO_4 samples, MS/MS fragmentation spectra of reaction products.

DOI: 10.1039/D1CP05427D

conditions. At the laboratory scale small quantities of HCN can be produced by the reaction of alkali cyanides with mineral acids. Besides the use of highly toxic precursors, this method is also disadvantageous because the resulting gas is contaminated by water and other impurities and needs complex purification procedures. To overcome these problems an innovative HCN production method was developed by using the more stable and less toxic AuCN as precursors and its reduction in a pure H_2 atmosphere at 523 K in presence of small Pd particles as catalyst. Following this route, high purity HCN can be produced in an ampoule directly connected through a vacuum line to the cell containing the solid of interest (previously outgassed at high temperature under high vacuum to desorb any surface contaminant) and dosed from the gas phase.

The interaction of HCN with the investigated solids and the formation of the reaction products was studied by IR spectroscopy in the 150-300 K temperature range which is compatible with the typical temperatures of interplanetary regions and comas surfaces.[29, 30] The composition of the reaction products was then determined, after their extraction with methanol, by high-resolution mass spectrometry (HR-MS), as outlined in the schematic workflow (**Fig. 1**).

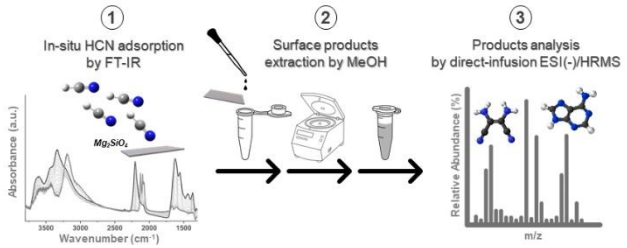

Figure 1. Schematic workflow: (1) in situ FT-IR investigation of the HCN adsorption and reactivity, (2) products extraction by methanol, (3) products identification by direct-infusion ESI(-)/HRMS.

Results and discussion

IR spectroscopy investigation of HCN interaction at the surface of model solids

The IR spectra obtained by interaction of gaseous HCN with CMS (panels B-B") and AMS (panels C-C") Mg-silicates and with the amorphous SiO_2 (panels A-A") and MgO (panels D-D") reference samples are compared in **Fig. 2**. Among the investigated solids, amorphous SiO_2 is the simplest in terms of chemical composition and surface structure. Indeed, after outgassing at high temperature only isolated Si-OH silanol groups, characterized by an IR absorption at 3747 cm^{-1} due to the ν(O-H) stretching mode, are present on its surface conferring to the solid weak Brønsted acid properties.[31] The interaction with HCN at 150 K (blue spectrum in panels A-A" of **Fig. 2**) leads to the erosion of the ν(O-H) band (negative signal at 3747 cm^{-1} in the background subtracted spectrum) and the formation of a new ν(O-H) broad band centered at 3475 cm^{-1}. Two additional absorptions are simultaneously formed at 3190 cm^{-1} and 2105 cm^{-1} due to the C-H and C≡N stretching modes of molecularly adsorbed HCN. The intensity of all the above manifestations is gradually reduced upon increasing the temperature from 150 K up to 300 K, while the signal of the free silanols is correspondingly restored. These results can be interpreted on the basis of formation of weak Si-OH···(HCN) hydrogen bonded complexes (see Zecchina *et al.*[32] and references therein) fully reversible upon increasing the sample temperature from 150 K to 300 K with no evidence of formation of other products. Indeed, the only manifestations observed in the spectrum at 300 K is the roto-vibrational contour of HCN gas, i.e. the C-H stretching mode centred at 3311 cm^{-1} and the first harmonic of the HCN bending vibration, centred at 1412 cm^{-1}.[33] The ν(C≡N) mode, expected at 2097 cm^{-1} for HCN in gas phase is too weak to be detected. This behaviour clearly shows the chemical inertness of SiO_2 towards HCN in our experimental conditions.

Spectral features ascribable to formation of Si-OH···(HCN) surface complexes are observed also in the spectra at 150 K of the HCN/CMS and HCN/AMS systems at ca. 2095 cm^{-1}. This is not surprising since Si-OH defective groups are expected to be present also at the surface of the siliceous portions of the CMS and AMS matrices.[24] Differently from SiO_2, in the spectra of the HCN/CMS and HCN/AMS systems a new band in the ν(C≡N) region is observed at ca. 2130 cm^{-1} (panels B' and C' in **Fig.2**). The presence of a similar signal also in the spectrum of the HCN/MgO system, where it is accompanied by an additional component at 2080 cm^{-1} (panel D' in **Fig. 2**), allows its assignment to the interaction of HCN with Mg-containing centers. The relative intensity of the 2130 cm^{-1} band progressively increases in the order CMS < AMS < MgO, suggesting its assignment to CN^- species[34] formed by HCN dissociation on $Mg^{2+}O^{2-}$ acid-base pairs, as shown in the first step of **Scheme 1**:

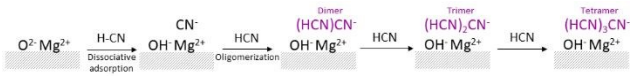

Scheme 1. Schematic representation of the initial stages of the complex HCN/MgO surface chemistry observed in this work. The chain reaction is initiated by the HCN dissociative adsorption on coordinatively unsaturated $Mg^{2+}O^{2-}$ acid-base pairs exposed at the surface of the MgO nanocrystals (represented by the grey areas). Subsequent nucleophilic attack of gaseous molecules by the adsorbed CN^- fragment leads to formation of negatively charged oligomeric species anchored to the surface.

The presence of a variety of exposed coordinatively unsaturated $Mg^{2+}O^{2-}$ acid-base pairs at the surface of nanocrystalline MgO (like the sample used in this study) is well established in the literature. Among them, the 3-fold coordinated species located at the corners of the MgO nanocrystals have been reported to be highly reactive, being able to heterolytically split the H_2 molecule at room temperature to give OH^- and Mg-hydrides,[35] as well as to form $(C_nO_{n+1})^{2-}$ oligomers by reaction of the strongly basic O^{2-} species with gaseous CO.[35, 36] It is assumed that the same species are the main responsible for the reactivity observed with HCN (see **Scheme 1**), although the participation $Mg^{2+}O^{2-}$ pairs in less defective positions (like at the edges or at the extended surfaces of the MgO nanocrystals) cannot be excluded *a priori*. The behaviour of the Mg_2SiO_4 samples (and the reactivity scale as compared to MgO) can be accounted for

View Article Online
DOI: 10.1039/D1CP05407D

by considering the structural properties of these materials (see **Fig. S1**). While AMS can be described as a random mixture of Mg^{2+} ions, $(MgO)_x$ polymers and monomeric SiO_4 or dimeric Si_2O_7 units, the bulk structure of CMS is represented by an ordinate distribution of negatively charged SiO_4 tetrahedra and intercalated isolated Mg^{2+} ions.[24-28] The expected presence of $Mg^{2+}O^{2-}$ pairs belonging to the $(MgO)_x$ clusters on AMS well accounts for the occurrence in the spectrum of the HCN/AMS system at 150 K of the 2130 cm^{-1} component already observed on MgO (blue lines in panels C' and D' of **Fig. 2**) and assigned to dissociatively adsorbed HCN (**Scheme 1**). The lower intensity of this component on AMS with respect to MgO is in full agreement with the lower concentration of the $Mg^{2+}O^{2-}$ pairs on the Mg-silicate as compared to pure MgO. The presence of the component at 2130 cm^{-1} also in the spectrum of HCN adsorbed at 150 K on CMS, although with low intensity, seems to confirm the hypothesis already advanced in previous studies[24] that low concentration $(MgO)_x$ moieties due to incomplete crystallization or surface rearrangements are also present on the crystalline Mg-silicate.

As evident in **Fig. 2**, the spectra of HCN adsorbed on the Mg-containing samples undergo dramatic changes when the temperature is allowed to freely rise to 300 K. In particular, all the manifestations discussed in the previous part associated to molecularly and dissociatively adsorbed HCN gradually disappear. In parallel we observe the growth of a broad and complex absorption at higher frequency covering the whole 2250-2150 cm^{-1} interval, which can be ascribed to the formation of oligomeric or more complex CN containing products.[37-39] Especially on AMS and MgO, the transformations are accompanied by the increase of broad absorption due to the progressive formation of new OH groups engaged in medium-strong hydrogen-bonding interactions. This observation further confirms the occurrence of a proton extraction from HCN or hydrogenated CN containing products by $Mg^{2+}O^{2-}$ acid-base pairs. Moreover, the presence of a narrow component superimposed to the broad ν(OH) band at ca. 3340 cm^{-1} is clear evidence of the formation also of N-H groups in the reaction products. The occurrence of a complex surface chemistry already at low temperature is further demonstrated by the growth in the 1750-1300 cm^{-1} region of a variety of bands compatible with the presence of functional groups like C=O, C=N, C-N, C=C, etc. and hence of complex reaction products.

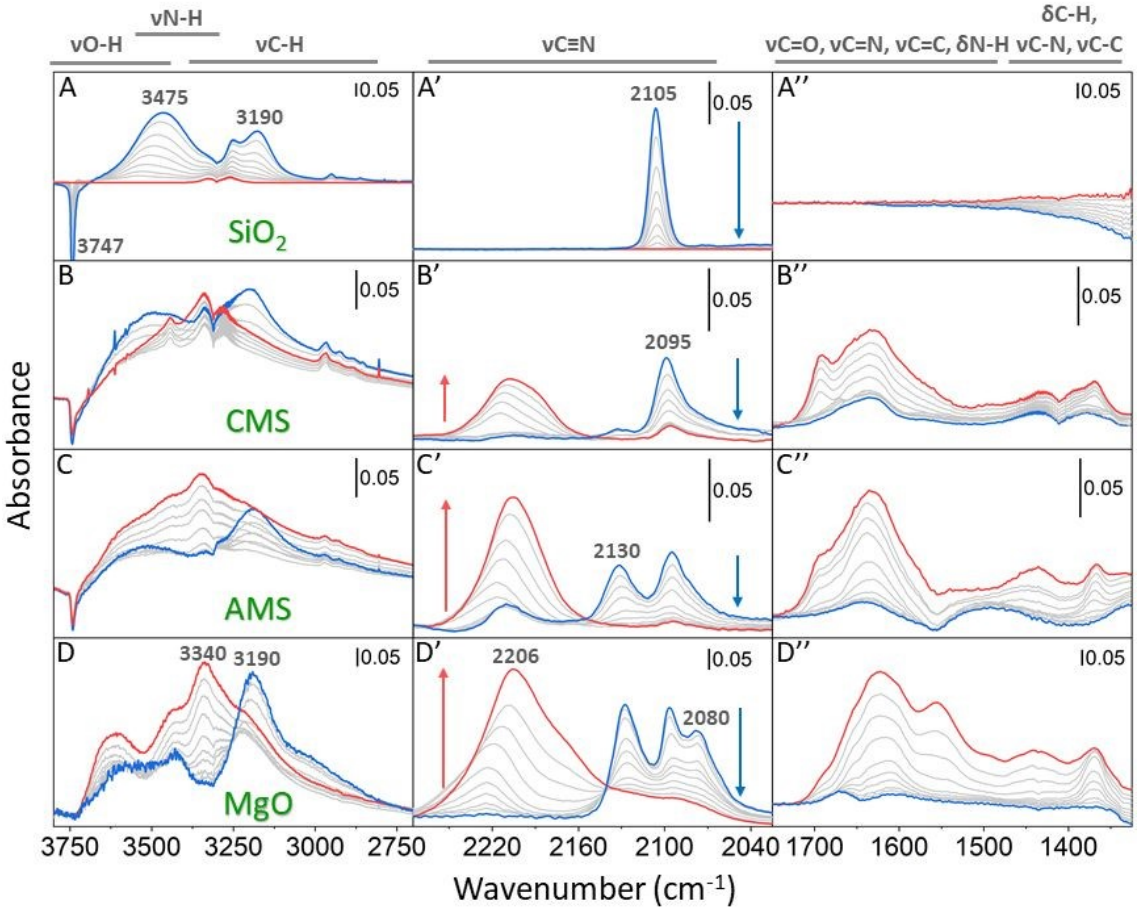

Figure 2. IR difference spectra obtained by interaction of gaseous HCN in the 150-300 K range with amorphous SiO2 (panels A-A''), CMS (panels B-B'), AMS (panels C-C'') and MgO (panels D-D''). In all the series the blue curve is the spectrum at 150 K, the grey lines the spectral sequence obtained by allowing the samples temperature to freely rise up to 300 K in HCN atmosphere and the red line the spectrum recorded after 10 min at 300 K. Before HCN adsorption all the solids where outgassed under high vacuum at high temperature (see SI for details) in order to remove adsorbed water and other surface contaminants. The contribution from the bare activated material has been subtracted from the reported spectra. The negative peaks belong to species which are consumed following the HCN/solid interaction, while the positive peaks to species which are formed.

High-resolution mass spectrometry analysis of the obtained species and data discussion

To achieve deeper insights into the nature of the final surface species, after the IR experiments, the samples were washed with methanol to extract the reaction products which were subsequently analysed by direct infusion high resolution mass spectrometry (HR-MS).

For the sake of brevity only the mass spectrum (ESI, negative mode) obtained on the most active solid (MgO) is reported in **Fig. 3**. Similar spectra were obtained on CMS and AMS, although with reduced absolute intensity (SI Appendix, **Fig. S2**).

The relative abundances of the different HCN reaction products for the different solids are compared in **Table 1**. The identification of the different products comes from ESI-MS/MS direct infusion data which allowed us to isolate and fragment each mass of interest (SI Appendix, **Table S1**, **Fig. S3**, and related comments for further details). The HR-MS spectra (**Fig. 3**) suggest the presence of three different families of products: $(HCN)_x$ oligomers, species with $(HCN)_x(CN)_2$ composition (coded in blue in the figure) and oxygen containing derivates of general formula $(HCN)_xO$ (in green). In the $(HCN)_x$ series, the most abundant products (see **Table 1**) are the aminomalonitrile trimer (AMN, m/z ≈ 80) and the diaminomaleonitrile tetramer (DAMN, m/z ≈ 107). This reactivity can be rationalized considering that the ability of bases to promote the HCN oligomerization by a nucleophilic mechanism in homogeneous conditions is well documented.[40, 41] For instance, dimerization readily occurs in ammonia solutions by reaction of undissociated HCN molecules with the strong CN^- nucleophile. The subsequent nucleophilic attack of the dimer by CN^- leads to the AMN trimer and, in cascade, to the DAMN tetramer.[42]

Yuasa *et al*.[43, 44] have shown that Mg-containing minerals like MgO (periclase) and $MgCO_3$ (magnesite) can play the same role as ammonia in catalysing the HCN oligomerization at liquid/solid interphases. Considering our IR data, we can conclude that in our Mg-containing samples AMN and DAMN are formed with a similar mechanism starting from adsorbed HCN dissociation on acid/base $O^{2-}Mg^{2+}$ surface couples (IR signals in the 2150-2050 cm^{-1} interval) and progressive HCN addition to form oligomers containing C≡N groups (IR signals in the 2250-2150 cm^{-1} interval) according to **Scheme 1**.

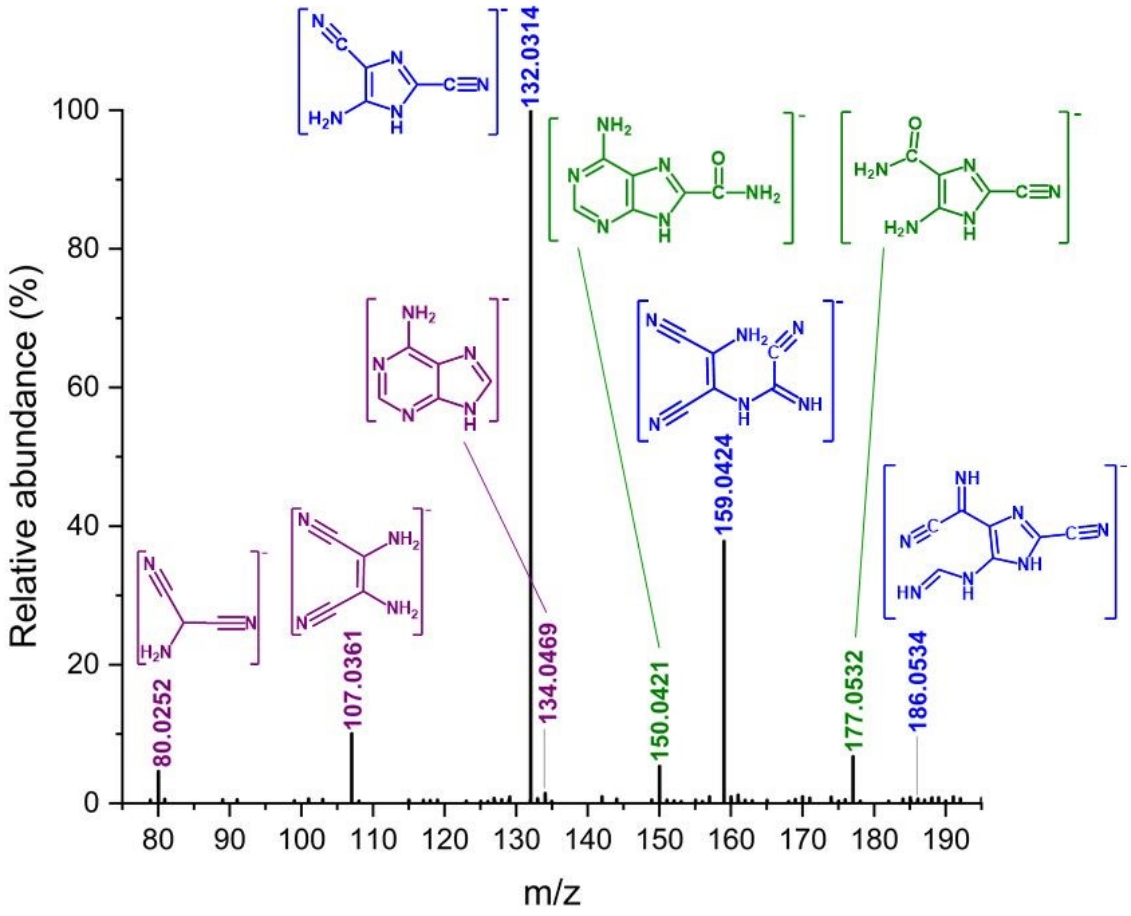

Figure 3. ESI-HRMS spectra of HCN/MgO reaction products after extraction with methanol. The m/z values of the most significant signals are shown together with the proposed structures of the corresponding product. The different colours identify different class of compounds: violet for (HCN)x oligomers, blue for $(HCN)_x(CN)_2$ and green for oxygenated $(HCN)_xO$ species.

View Article Online
DOI: 10.1039/D1CP05407D

Table 1. Ions identified from direct infusion ESI-HRMS spectra in Fig. 3, including formulae, mass measurement errors, and relative abundance (normalized on related base peak) of extracted solutions from MgO, AMS and CMS.

HCN species	Chemical Formula $[M-H]^-$	Measured m/z	Theoretical m/z	Δppm	Relative Abundance *base peak		
					MgO	AMS	CMS
$(HCN)_3$	$[C_3H_2N_3]^-$	80.0252	80.0254	-2.630	4.62	2.75	3.28
$(HCN)_4$	$[C_4H_3N_4]^-$	107.0361	107.0363	-1.677	10.1	100*	100*
$(HCN)_5$	$[C_5H_4N_5]^-$	134.0469	134.0472	-2.227	1.45	0.340	0.150
$(HCN)_3(CN)_2$	$[C_5H_2N_5]^-$	132.0314	132.0316	-1.579	100*	32.5	0.600
$(HCN)_4(CN)_2$	$[C_6H_3N_6]^-$	159.0424	159.0425	-0.676	37.8	13.1	0.710
$(HCN)_5(CN)_2$	$[C_7H_4N_7]^-$	186.0534	186.0534	0.126	0.410	3.96	0.280
$(HCN)_5O$	$[C_5H_4ON_5]^-$	150.0421	150.0421	-0.421	5.34	5.47	0.900
$(HCN)_6O$	$[C_6H_5ON_6]^-$	177.0532	177.0530	0.835	6.76	1.58	0.120

The presence of a signal m/z ≈ 134 easily assigned to $(HCN)_5$ pentamers is particularly relevant since a molecule having this composition is the adenine nucleobase. The formation of adenine from HCN in ammonia solutions has been reported to occur under UV irradiation as well as in the dark upon heating.[40] In both cases it has been proposed that adenine is the product of reactions chains initiated by the DAMN. Among the reaction paths proposed for the chemical transformation of DAMN into adenine,[45] the mechanism of Voet and Schwartz,[46] which does not require the presence of UV irradiation, is in nice agreement with the reaction products composition revealed by our HR-MS results. This suggests that a reaction mechanism similar to that proposed by Voet and Schwartz for the HCN/NH_3 homogenous system, and illustrated in a simplified version in **Scheme 2**, could operate for the HCN/solid interaction in our heterogeneous conditions. Following the mechanism of **Scheme 2**, the chains of reactions leading from DAMN to adenine is initiated by the formation of the $(HCN)_4(CN)_2$ (a) intermediate which can then rearrange to give imidazole (a') or purine (a'') isomeric products. The (a') and (a'') intermediates can further evolve following two different pathways finally leading to imidazole compounds (d) (pathway A in **Scheme 2**) and to adenine (f) (pathway B in **Scheme 2**). Both reactive routes lead also to the formation of oxygenated species (e, d) which, in our conditions (i.e., pure HCN and highly dehydroxylated samples), can only involve the participation of the highly coordinatively unsaturated O^{2-} surface sites[35] responsible for HCN dissociation and for the consequent formation of OH^- species.

Concerning the relative abundance of the products in the different samples (**Table 1**), the most abundant species for HCN/MgO are $(HCN)_3(CN)_2$ at m/z 132 (base peak) and $(HCN)_4(CN)_2$ at m/z 159 suggesting that the HCN reactivity preferentially evolves via pathway A of **Scheme 2** to form species with imidazole structure.

Conversely, for the Mg-silicates the DAMN represents the most abundant species: in AMS we can also detect a significant amount of $(HCN)_3(CN)_2$, while on CMS complex reaction products seems to be rare.

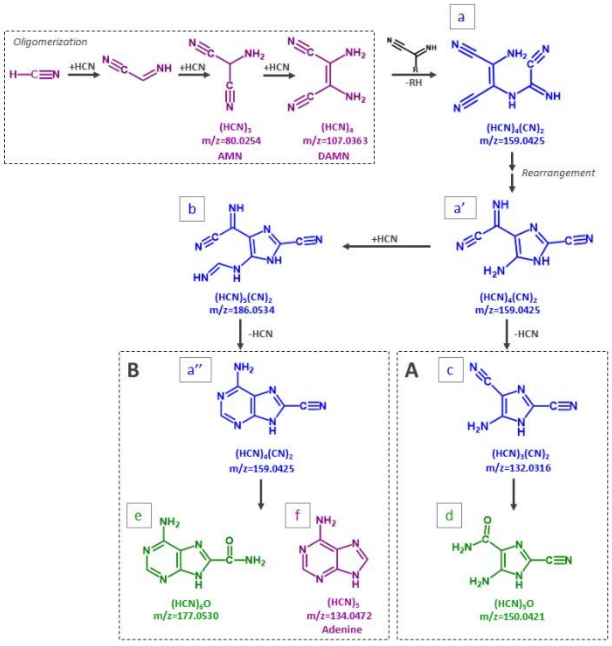

Scheme 2. Simplified version of the Voet and Schwartz mechanism[43] describing the formation of adenine from HCN. The m/z values of the involved species are reported for sake of comparison with the masses identified in the ESI (-)/HRMS spectra of Fig. 3. The same colour coding of Fig. 3 is used here to individuate different classes of products. A similar reaction pathway is hypothesized for the formation of adenine by reaction of gaseous HCN at the MgO, AMS and CMS surfaces.

These observations are in agreement with the different surface reactivity already revealed by IR and strictly correlated to the presence of strongly basic O^{2-} sites.[24] Finally, it is worth to underline that the species detected by HR-MS are fully compatible with the IR spectra obtained for the HCN/CMS, HCN/AMS and HCN/MgO systems (**Fig. 2**). Indeed, in the 1650-1500 cm^{-1} region we can recognize signals due to ν(C=N)

View Article Online
DOI: 10.1039/D1CP05407D

stretching of imine-like species, to ν(C=C) aromatic stretching in ring structures and to δ(NH/NH_2) bending of amine groups. The presence of N-H species is further testified by related ν(N-H) absorption at ca. 3340 cm^{-1}. In addition, the bands at 1450-1350 cm^{-1} can be assigned to ν(C-C) and ν(C-N) ring stretching modes of N-bearing heteroaromatic or heterocyclic compounds, while the ν(C=O) mode of the oxygenated key species (e) and (d) in **Scheme 2** appears as a shoulder at ca. 1700 cm^{-1}.

Conclusions

In summary, to the best of our knowledge, our results are the first evidence that the reactivity of hydrogen cyanide to form complex products like those observed in solution or at solid/liquid interphases can be reproduced at the gas/solid interphase, in very mild conditions and without external energy sources (UV irradiation or electrical discharges). The *in situ* IR investigation of the adsorption of HCN at low temperature on Mg-containing model minerals and of the subsequent reactivity allowed to highlight the key role of surface basicity. In particular, the presence of Mg^{2+}-O^{2-} pairs appeared to be crucial to initiate a complex surface chemistry by preliminary HCN dissociation. The HR-MS analysis of the extracted products allowed us to identify the presence among the reaction products of HCN oligomers (mainly the AMN trimer and the DAMN tetramer) and as well as of imidazole and purine compounds. The evidence of the formation of the adenine nucleobase is of considerable importance because of the implications in field of the prebiotic chemistry in the astrophysical contexts. Indeed, our experiments are compatible with a primordial scenario in which HCN in gaseous form comes directly into contact with the surface of Mg-silicates, which are abundant in the core of the interstellar medium particles as well as the main constituent of the core of the comets, like the 67/P. It is worth mentioning that the range of temperature explored in the present work brackets the temperatures measured at the surface of northern latitudes of 67/P comet, reaching values as high as 230 K.[29] Due to the relevance of both HCN and amorphous and crystalline silicates in the comet's compositions,[30] the present results may guide our understanding of the complex chemical processes occurring not only at the interstellar core grains but also in these astronomical bodies which are relevant for bringing molecular building blocks of the kind observed in the present experiments to large planetary bodies.

Thus, our contribution can stimulate new investigations about the role of gas-surface interactions involving HCN in the abiotic formation of nucleobases both in endogenous and exogenous prebiotic conditions.

Data availability

Further experimental data are available in the ESI.†

Author Contributions

Conceptualization: R.S, D.S, P.U., G.S., and L.M.; data curation: R.S, M.P., D.S., G.S., and L.M.; formal analysis: F.B, and M.S.; funding acquisition: P.U., investigation: R.S, M.P., D.S., G.S., and L.M., methodology: R.S, D.S, G.S., and L.M.; validation: R.S, D.S, P.U., and G.S., writing – original draft: R.S., D.S., P.U., G.S., and L.M.

Conflicts of interest

There are no conflicts to declare.

Acknowledgements

P.U. acknowledge the Marie Sklodowska-Curie project "Astro-Chemical Origins" (ACO), grant agreement No 811312 for discussion with members of the team (Cecilia Ceccarelli and Nadia Balucani). Support from the Italian MIUR (PRIN 2020, "Astrochemistry beyond the second period elements", Prot. 2020AFB3FX) is gratefully acknowledged.

Notes and References

1. J. Orò, *Biochem. Biophys. Res. Commun.* , 1960, **2**, 407-412.
2. M. Ruiz-Bermejo, M. P. Zorzano and S. Osuna-Esteban, *Life (Basel)*, 2013, **3**, 421-448.
3. M. P. Callahan, K. E. Smith, H. J. Cleaves, 2nd, J. Ruzicka, J. C. Stern, D. P. Glavin, C. H. House and J. P. Dworkin, *Proc Natl Acad Sci U S A*, 2011, **108**, 13995-13998.
4. Z. Martins, *Life (Basel)*, 2018, **8**, 28.
5. L. E. Snyder and D. Buhl, *Astrophys. J.* , 1971, **163**, L47.
6. A. T. Tokunaga, S. C. Beck, T. R. Geballe, J. H. Lacy and E. Serabyn, *Icarus*, 1981, **48**, 283-289.
7. A. Marten, D. Gautier, T. Owen, D. B. Sanders, H. E. Matthews, S. K. Atreya, R. P. J. Tilanus and J. R. Deane, *Astrophys. J.* , 1993, **406**, 285.
8. S. Rodgers and S. Charnley, *Astrophys. J. Letter.*, 2009, **501**, L227.
9. A. Adriani, B. M. Dinelli, M. López-Puertas, M. García-Comas, M. L. Moriconi, E. D'Aversa, B. Funke and A. Coradini, *Icarus*, 2011, **214**, 584-595.
10. D. M. Graninger, E. Herbst, K. I. Öberg and A. I. Vasyunin, *Astrophys. J.* , 2014, **787**, 74.
11. J.-C. Loison, V. Wakelam and K. Hickson, *Mon. Notices Royal Astron. Soc.*, 2014, **443**, 398-410.
12. E. Lellouch, M. Gurwell, B. Butler, T. Fouchet, P. Lavvas, D. F. Strobel, B. Sicardy, A. Moullet, R. Moreno, D. Bockelée-Morvan, N. Biver, L. Young, D. Lis, J. Stansberry, A. Stern, H. Weaver, E. Young, X. Zhu and J. Boissier, *Icarus*, 2017, **286**, 289-307.
13. R. M. Hazen, D. Papineau, W. Bleeker, R. T. Downs, J. M. Ferry, T. J. McCoy, D. A. Sverjensky and H. Yang, *Am. Mineral.*, 2008, **93**, 1693-1720.
14. T. Henning, *Ann. Rev. Astron. Astrophys.*, 2010, **48**, 21-46.
15. C. Jäger, J. Dorschner, H. Mutschke, T. Posch and T. Henning, *Astron. Astrophys.*, 2003, **408**, 193-204.

16. R. M. Hazen and D. A. Sverjensky, *Cold Spring Harb Perspect Biol*, 2010, **2**, a002162.
17. E. Herbst and E. F. van Dishoeck, *Ann. Rev. Astron. Astrophys.*, 2009, **47**, 427-480.
18. R. Saladino, C. Crestini, S. Pino, G. Costanzo and E. Di Mauro, *Phys Life Rev*, 2012, **9**, 84-104.
19. H. L. Barks, R. Buckley, G. A. Grieves, E. Di Mauro, N. V. Hud and T. M. Orlando, *Chembiochem*, 2010, **11**, 1240-1243.
20. R. Saladino, E. Carota, G. Botta, M. Kapralov, G. N. Timoshenko, A. Y. Rozanov, E. Krasavin and E. Di Mauro, *Proc Natl Acad Sci U S A*, 2015, **112**, E2746-2755.
21. L. Rotelli, J. M. Trigo-Rodriguez, C. E. Moyano-Cambero, E. Carota, L. Botta, E. Di Mauro and R. Saladino, *Sci Rep*, 2016, **6**, 38888.
22. Y. Oba, Y. Takano, H. Naraoka, N. Watanabe and A. Kouchi, *Nat Commun*, 2019, **10**, 4413.
23. M. A. Corazzi, D. Fedele, G. Poggiali and J. R. Brucato, *Astron. Astrophys.*, 2020, **636**, A63.
24. M. Signorile, L. Zamirri, A. Tsuchiyama, P. Ugliengo, F. Bonino and G. Martra, *ACS Earth and Space Chem.*, 2020, **4**, 345-354.
25. S. Kohara, K. Suzuya, K. Takeuchi, C. K. Loong, M. Grimsditch, J. K. R. Weber, J. A. Tangeman and T. S. Key, *Science*, 2004, **303**, 1649-1652.
26. S. Kohara, J. Akola, H. Morita, K. Suzuya, J. K. R. Weber, M. C. Wilding and C. J. Benmore, *Proc. Natl. Acad. Sci. U.S.A.*, 2011, **108**, 14780.
27. L. Zamirri, M. Corno, A. Rimola and P. Ugliengo, *ACS Earth and Space Chem.*, 2017, **1**, 384-398.
28. D. Yamamoto and S. Tachibana, *ACS Earth and Space Chem.*, 2018, **2**, 778-786.
29. F. Tosi, F. Capaccioni, M. T. Capria, S. Mottola, A. Zinzi, M. Ciarniello, G. Filacchione, M. Hofstadter, S. Fonti, M. Formisano, D. Kappel, E. Kührt, C. Leyrat, J. B. Vincent, G. Arnold, M. C. De Sanctis, A. Longobardo, E. Palomba, A. Raponi, B. Rousseau, B. Schmitt, M. A. Barucci, G. Bellucci, J. Benkhoff, D. Bockelée-Morvan, P. Cerroni, J. P. Combe, D. Despan, S. Erard, F. Mancarella, T. B. McCord, A. Migliorini, V. Orofino and G. Piccioni, *Nat. Astron.*, 2019, **3**, 649-658.
30. V. Dorofeeva, *Sol. Syst. Res.*, 2020, **54**, 96-120.
31. K. Hadjiivanov, *Adv. Catal.*, 2014, **57**, 99-318.
32. A. Zecchina, G. Spoto and S. Bordiga, in *Handbook of Vib. Spectrosc.*, ed. J. M. C. a. P. R. Griffiths, 2006, vol. 4, pp. 3043-3071.
33. K. Nakamoto, 2006, DOI: 10.1002/9780470027325.s4104.
34. A. M. C. a. A. I. C. Tsyganenko, *Phys Chem Chem Phys*, 2010, **12**, 6307-6308.
35. G. Spoto, E. N. Gribov, G. Ricchiardi, A. Damin, D. Scarano, S. Bordiga, C. Lamberti and A. Zecchina, *Prog. Surf. Sci.*, 2004, **76**, 71-146.
36. A. Zecchina, S. Coluccia, G. Spoto, D. Scarano and L. Marchese, *Journal of the Chemical Society, Faraday Transactions*, 1990, **86**, 703-709.
37. V. Vuitton, J. Y. Bonnet, M. Frisari, R. Thissen, E. Quirico, O. Dutuit, B. Schmitt, L. Le Roy, N. Fray, H. Cottin, E. Sciamma-O'Brien, N. Carrasco and C. Szopa, *Faraday Discuss*, 2010, **147**, 495-508; discussion 527-452.
38. M. Ruiz-Bermejo, J. L. de la Fuente and M. R. Marín-Yaseli, *J. Anal. Appl. Pyrolysis*, 2017, **124**, 103-112.
39. M. Ruiz-Bermejo, J. L. de la Fuente, J. Carretero-Gonzalez, L. Garcia-Fernandez and M. R. Aguilar, *Chem. Eur. J.*, 2019, **25**, 11437-11455.
40. J. P. F. O. Sanchez, L.E. Orgel, *J. Mol. Biol.* , 1967, **30**, 223-253.
41. D. B. D. J. P. Ferris, A. P. Lobo, *J. Mol. Biol.* , 1973, **74**, 511-518.
42. J. D. W. J. P. Ferris, T. J. Ryan, A. P. Lobo, D. B. Donner, *Orig. Life Evol. Biosph.* , 1974, **5**, 153-157.
43. J. O. S. Yuasa, in *Cosmochemical Evolution and the Origins of Life*, ed. D. Springer, 1974, pp. 295-299.
44. M. I. S. Yuasa, *Geochem. J.* , 1977, **11**, 247-252.
45. M. Yadav, R. Kumar and R. Krishnamurthy, *Chem Rev*, 2020, **120**, 4766-4805.
46. A. W. S. A.B. Voet, *Bioorg. Chem.* , 1983, 8-17.